Inorg. Chem. **2006**, *45*, 5321–5327

On the Structure and Spin States of Fe(III)-EDDHA Complexes

Mar Gómez-Gallego,*,† Israel Fernández,† Daniel Pellico,† Ángel Gutiérrez,‡ Miguel A. Sierra,*,† and Juan J. Lucena§

Departamentos de Química Orgánica y Química Inorgánica, Facultad de Química, Universidad Complutense, 28040 Madrid, Spain, and Sección de Química Agrícola. Facultad de Ciencias, CVII, Universidad Autónoma, 28049 Madrid, Spain

Received December 2, 2005

DFT methods are suitable for predicting both the geometries and spin states of EDDHA-Fe(III) complexes. Thus, extensive DFT computational studies have shown that the *racemic*-Fe(III) EDDHA complex is more stable than the meso isomer, regardless of the spin state of the central iron atom. A comparison of the energy values obtained for the complexes under study has also shown that high-spin ($S = 5/2$) complexes are more stable than low-spin ($S = 1/2$) ones. These computational results matched the experimental results of the magnetic susceptibility values of both isomers. In both cases, their behavior has been fitted as being due to isolated high-spin Fe(III) in a distorted octahedral environment. The study of the correlation diagram also confirms the high-spin iron in complex **2b**. The geometry optimization of these complexes performed with the standard 3-21G* basis set for hydrogen, carbon, oxygen, and nitrogen and the Hay-Wadt small-core effective core potential (ECP) including a double-ξ valence basis set for iron, followed by single-point energy refinement with the 6-31G* basis set, is suitable for predicting both the geometries and the spin-states of EDDHA-Fe(III) complexes. The presence of a high-spin iron in Fe(III)-EDDHA complexes could be the key to understanding their lack of reactivity in electron-transfer processes, either chemically or electrochemically induced, and their resistance to photodegradation.

Introduction

The geometry and electronic structure of a transition-metal complex are interrelated properties and dictate both the physical characteristics and chemical reactivity of a given molecule.[1] In the case of Fe(II) and Fe(III) complexes, the influence of the spin state of the metal in determining the stereochemistry and geometric properties of the complex is a frequent matter of study and has been particularly well-established in iron porphyrins.[2] The relationship between the structure and properties has also been a subject of interest in the case of the Fe(III) complexes of EDDHA (ethylenediamine *N*,*N*′-bis(2-hydroxy)phenylacetic acid **1**, Chart 1). This is one of the most-efficient iron chelating agents employed to relieve iron chlorosis in plants[3,4] and also has applications in positron emission tomography[5] and as a paramagnetic contrast agent for magnetic resonance imaging.[6]

Chart 1

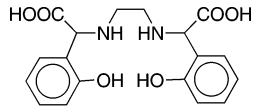

1

Because two stereogenic centers are present, EDDHA **1** exists in two diastereomeric forms, a meso (*RS*,*SR*) isomer and a racemic (*RR*,*SS*) pair. The crystal structures[7] of

* To whom correspondence should be addressed. E-mail: margg@quim.ucm.es (M.G.-G.); sierraor@quim.ucm.es (M.A.S.).
† Departamento de Química Orgánica, Universidad Complutense.
‡ Departamento de Química Inorgánica, Universidad Complutense.
§ Universidad Autónoma.

(1) (a) Nelson, S. M. In *Comprehensive Coordination Chemistry*; Wilkinson, G., Gillard, R. D., McCleverty, J. A., Eds.; Pergamon: Oxford, U.K., 1987; Vol. 4, pp 217−276. Two recent examples: (b) Iwakura, I.; Ikeno, T.; Yamada, T. *Angew. Chem., Int. Ed.* **2005**, *44*, 2524. (c) Griesbeck, A. G.; Abe, M.; Bondock S. *Acc. Chem. Res.* **2004**, *37*, 919.
(2) (a) Scheidt, W. R.; Reed, C. A. *Chem. Rev.* **1981**, *81*, 543. (b) Rath, S. P.; Olmstead, M.; Balch, A. L. *J. Am. Chem. Soc.* **2004**, *126*, 6379. (c) Yatsunik, L. A.; Walker, F. A. *Inorg. Chem.* **2004**, *43*, 4341. (d) Hawrelak, E. J.; Bernskoetter, W. H.; Lobkovsky, E.; Yee, G. T.; Bill, E.; Chirik, P. J. *Inorg. Chem.* **2005**, *44*, 3103.
(3) (a) Yunta, F.; García-Marco, S.; Lucena, J. J.; Gómez-Gallego, M.; Alcázar, R.; Sierra, M. A. *Inorg. Chem.* **2003**, *42*, 5412. (b) Sierra, M. A.; Gómez-Gallego, M.; Alcázar, R.; Lucena, J. J.; Yunta, F.; García-Marco, S. *Dalton Trans.* **2004**, 3741.
(4) (a) Mengel, K.; Kirby, E. A.; Kosegarten, H.; Appel, T. In *Principles of Plant Nutrition*; Kluwer Academic: Dordrecht, The Netherlands, 2001; pp 553−571. (b) Chen, Y.; Barak, P. *Adv. Agron.* **1982**, *5*, 217. (c) Chaney, R. L. *J. Plant. Nutr.* **1984**, *7*, 47.

10.1021/ic0520723 CCC: $33.50
Published on Web 06/16/2006

Chart 2

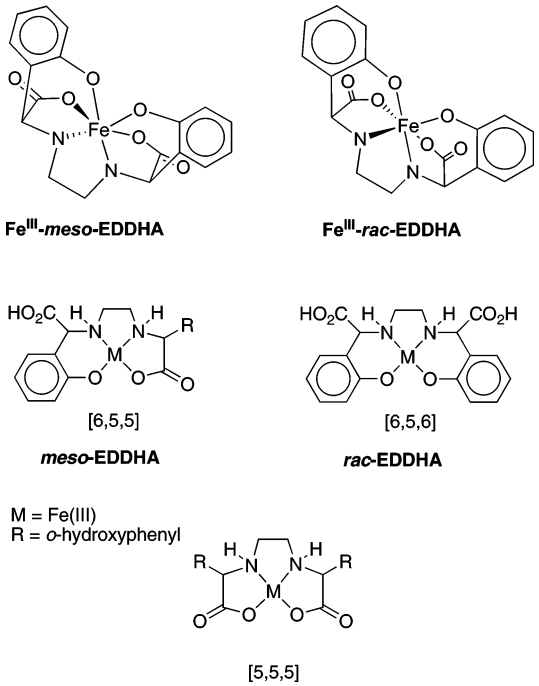

hexacoordinate *meso*- and *racemic*-Na[Fe(III)-EDDHA] show that although both complexes have an octahedral coordination environment for the metal, the meso and racemic ligands are in different arrangements within the complex. Thus, considering the equatorial plane of the complexes, the meso form has a [6,5,5] arrangement with one carboxylate group and one phenoxy group occupying the axial positions, whereas the racemic isomer shows a [6,5,6] arrangement with the two carboxylates axially placed (Chart 2).[8] Although the [5,5,5] arrangement with the two phenoxy groups on the axial positions is also possible for the racemic Fe(III) complex, this structure has not been found in the solid state. Both the *racemic*- and *meso*-EDDHA Fe(III) chelates are very stable, though greater stability has been found for the racemic complex compared to the meso form (log $K_{ML} = 35.0$ versus log $K_{ML} = 33.28$).[3,8a]

The differences observed in the stability of both Fe(III) complexes have been ascribed almost entirely to differences in coordination geometry.[9] Thus, an early work by Bernauer[10] proposed that the greater stability of the [6,5,6] Fe(III) *racemic*-EDDHA complex is a consequence of the more-favorable octahedral geometry achieved by placement of the six-membered chelate rings (with the greater bite angle) in the equatorial plane defined by the ethylenediamine ring. This argument also explains the absence of the [5,5,5] arrangement in the crystalline form. Since this preliminary work, no other attempts have been made to determine why *racemic*-EDDHA leads to more-stable Fe(III) complexes than the meso isomer. On the other hand, the influence of the spin state of the central iron atom on the geometry and properties of such complexes has not been yet considered.

Although Fe(III)-EDDHA complexes are the most widely used iron fertilizers, the mechanism of iron transfer from these chelates to strategy I plants (dicots and nongrass monocots) is still a subject of debate. In a recent study,[11] we have proposed a model for understanding their behavior toward the enzyme ferric chelate reductase. From this model, the lack of reactivity of Fe(III)-EDDHA in electron-transfer (ET) reactions (either chemically or photochemically induced) is related to the very negative reduction potential of the close octahedral complex ($E_{pc} = -0.56$ V, pH 7.1). The opening of a coordination site results in the lowering of the reduction potential, rendering these complexes prone to the action of the enzyme. For a fuller understanding of the mechanism of Fe uptake by strategy I plants, it was necessary to explore the structure of these complexes, relying on the suitability of computational DFT models to study both their geometries and spin states.

The relationship between the spin state of the iron and the behavior of the complex in ET processes has been established in Fe(III) porphyrins.[12] Thus, studies carried out in porphyrin-based donor−bridge−acceptor systems show that whereas the reactivity of low-spin ($S = 1/2$) Fe(III) porphyrin acceptors is dominated by ET, the corresponding high-spin ones ($S = 5/2$) are reluctant to take part in electron-transfer reactions; their deactivation occurs only by intersystem crossing. Considering these precedents, the above-mentioned properties of Fe(III)-EDDHA complexes could be directly related to the spin state of the central iron. In this paper, we report an exhaustive DFT study of *racemic*- and *meso*-Fe(III)-EDDHA complexes, considering both high- and low-spin states for the Fe(III) atom, as well as the different coordination geometries. The computational results will be compared with experimental data to estimate the accuracy of our models and, therefore, their suitability for further investigations.[13]

Experimental and Computational Methods

All the calculations reported in this paper were obtained with the GAUSSIAN 98 suite of programs.[14] They were performed using

(5) See for example: (a) Gaber, B. P.; Miskowski, V.; Spiro, T. G. *J. Am. Chem. Soc.* **1974**, *96*, 6868. (b) Peccoraro, V. L.; Harris, W. R.; Carrano, C. J.; Raymond, K. N. *Biochemistry* **1981**, *20*, 7033. (c) Peccoraro, V. L.; Bonadies, J. A.; Marrese, C. A.; Carrano, C. J. *J. Am. Chem. Soc.* **1984**, *106*, 3360. (d) Patch, M. G.; Simolo, K. P.; Carrano, C. J. *Inorg. Chem.* **1983**, *22*, 2630.

(6) Lauffer, R. B.; Vincent, A. C.; Padnamabhan, S.; Meade, T. J. *J. Am. Chem. Soc.* **1987**, *109*, 2216.

(7) Bailey, N. A.; Cummins, D.; McKenzie, E. D.; Worthington, J. M. *Inorg. Chim. Acta* **1981**, *50*, 111.

(8) a) Bannochie, C. J.; Martell, A. E. *Inorg. Chem.* **1991**, *30*, 1385. (b) Bannochie, C. J.; Martell, A. E. *J. Am. Chem. Soc.* **1989**, *111*, 4735.

(9) . The two free ligands have the same basicity (pK_a *racemic*-EDDHA 38.0 and pK_a *meso*-EDDHA 37.9) (see ref 8b); therefore, the differences in stabilities arise from the different geometries for both complexes.

(10) Bernauer, K. *Top. Curr. Chem.* **1976**, *65*, 1.

(11) Gómez-Gallego, M.; Pellico, D.; Ramírez-López, P.; Mancheño, M. J.; Romano, S.; de la Torre, M. C.; Sierra, M. A. *Chem.—Eur. J.* **2005**, *11*, 5997.

(12) Petterson, K.; Kilsa, K.; Martensson, J.; Albinsson, B. *J. Am. Chem. Soc.* **2004**, *126*, 6710.

(13) The Fe(II)-EDDHA complex is considerably less stable than the Fe(III) counterpart (log $K_{ML} = 15.3$, see: Lyndsay, L. *Chemical Equilibria in Soils*; Wiley: New York, 1979; pp 242) and has not been isolated. In consequence, there is no information available about the corresponding racemic and meso forms. Studies regarding the geometry and energy of these complexes as well as the relationship between the low stability of these complexes and their role in the iron uptake by dicotyledonous plants are now in progress and will be reported in due time.

the three-parameter exchange functional of Becke in conjunction with the gradient corrected correlation functional of Lee, Yang, and Parr.[15] Geometry optimization calculations were performed with the standard 3-21G*[16] basis set for hydrogen, carbon, oxygen, and nitrogen and the Hay-Wadt small-core effective core potential (ECP) including a double-ξ valence basis set[17] for iron (LanL2DZ keyword), followed by single-point energy refinement with the 6-31G* basis set. This protocol is designated as B3LYP/6-31G*&LanL2DZ//B3LYP/3-21G*&LanL2DZ. Zero point vibrational energy (ZPVE) corrections have been computed at the B3LYP/6-31G*&LanL2DZ level and have not been corrected. Stationary points were characterized by frequency calculations[18] and have positive defined Hessian matrixes.

The bulk magnetic susceptibility of samples of *meso*- and *racemic*-Na[Fe(III)-EDDHA] complexes has been measured using a SQUID magnetometer MPMS XL-5 manufactured by Quantum Design. The temperature dependence of the magnetization in the 2−300 K range was recorded using a constant magnetic field of 0.5 T. The experimental data have been corrected for the magnetization of the sample holder and for atomic diamagnetism as calculated from the known Pascal's constants. The samples of *meso*- and *racemic*-Na[Fe(III)-EDDHA] complexes were prepared as sodium salts from the pure ligands and ferric chloride in basic medium following the previously reported procedure.[7]

Results and Discussion

The DFT structures of the racemic and meso anions Fe(III)-EDDHA in low-spin ($S = 1/2$), **2a** and **3a**, and high-spin ($S = 5/2$), **2b** and **3b**, states as well as some selected optimized geometrical parameters, are shown in Figure 1. All complexes have a distorted octahedral geometry but, regardless of the spin state of the iron, racemic six-coordinate complexes **2a** and **2b** have the iron atom in a more symmetric environment than their meso counterparts **3a** and **3b**. In fact, the crystal structure of the racemic complex[7] shows the iron located on a 2-fold axis, whereas the meso form has no local symmetry imposed on it.

Details of the mean angles and bond distances obtained through DFT calculations are given in Table 1. The calculated bond distances and angles for complexes **2b** and **3b** are very similar to those of the X-ray data,[7] which suggests that the reported structures correspond to high-spin *racemic*- and *meso*-Fe(III)-EDDHA complexes.

The relationship between the geometry and the stereochemistry with the spin state of the Fe(III) center has been well-established in hexacoordinated iron complexes.[2] As is shown in Figure 1, the larger size of the high-spin Fe(III) has a noticeable effect in the complex geometry, as all the distances between the Fe and the N and O coordination sites are clearly elongated in high-spin ($S = 5/2$) complexes. Thus, when comparing low-spin and high-spin Fe(III) racemic complexes **2a** and **2b**, it can be observed that the increase in the size of the metal in high-spin ($S = 5/2$) complex **2b** causes the enlargement of the Fe−O3 and Fe−O4 distances in the equatorial plane (0.015 Å) and has a dramatic effect on the in-plane Fe−N distances (0.218 Å). The increase in the length of the Fe−O distances with the carboxylates in the axial plane is 0.099 Å, in accordance with the reported observation that the occupation of the d_{z^2} orbital in high-spin hexacoordinated complexes causes a lengthening of the axial iron−ligand bonds by ≥ 0.1 Å.[2]

The same effect is observed in meso complexes **3a** and **3b**. Again, the Fe−N equatorial distances are most affected by an increase in the metal size, and enlargements of 0.227 and 0.218 Å, respectively, are observed in high-spin ($S = 5/2$) complex **3b**. The Fe−O distances of axial and equatorial carboxylates also increase (0.127 and 0.045 Å, respectively), and finally, the Fe−O axial and equatorial phenolates are affected to a lesser extent (0.058 and 0.017 Å, respectively), though the axial distance is always the more elongated one.

The larger size of the high-spin iron induces a distortion in the coordination cavity, as can be seen by the higher values for the angles in the equatorial plane relative to those found for the low-spin derivatives This expansion produces a displacement of the iron atom out of the equatorial plane in the meso isomer of 0.13 Å in the crystal structure (0.076 Å calculated for **3b**). No displacement is observed for the racemic isomer **2b**, because the iron atom is located on a 2-fold axis; the nitrogen and oxygen equatorial atoms are, however, displaced from the mean plane by 0.054 and 0.049 Å, respectively, giving N−Fe−O angles around 165° instead of the close linearity expected for low-spin derivative **2a**. The shift of the core atoms on changing the spin of the iron can be observed in Figure 2.

To establish the relative stabilities of high- and low-spin complexes **2** and **3**, we have calculated their relative energies (kcal/mol) according to the procedure described in the Computational Methods section. The results shown in Figure 3 indicate that high-spin ($S = 5/2$) Fe(III) complexes **2b** and **3b** have considerably lower energy than the corresponding low-spin ones **2a** and **3a** ($\Delta E = 5.32$ and 5.29 kcal/mol, respectively). The higher stability of the high-spin state can also be derived from the closer DFT-optimized Fe−N and Fe−O bond distances relative to the experimental values for both the racemic and meso forms.[7]

The energy diagram also shows that for a given spin state of the iron, racemic complex **2** is always more stable than meso form **3** ($\Delta E = 4.72$ kcal/mol in high-spin complexes and $\Delta E = 4.69$ kcal/mol in low-spin complexes). The higher stability of *racemic*-Fe(III)-EDDHA compared to the meso

(14) Frisch, M. J.; Trucks, G. W.; Schlegel, H. B.; Scuseria, G. E.; Robb, M. A.; Cheeseman, J. R.; Zakrzewski, V. G.; Montgomery, J. A., Jr.; Stratmann, R. E.; Burant, J. C.; Dapprich, S.; Millam, J. M.; Daniels, A. D.; Kudin, K. N.; Strain, M. C.; Farkas, O.; Tomasi, J.; Barone, V.; Cossi, M.; Cammi, R.;. Mennucci, B.; Pomelli, C.; Adamo, C.; Clifford, S.; Ochterski, J.; Petersson, G. A.; Ayala, P. Y.; Cui, Q.; Morokuma, K.; Rega, N.; Salvador, P.; Dannenberg, J. J.; D Malick, D. K.; Rabuck, A. D.; Raghavachari, K.; Foresman, J. B.; Cioslowski, J.; Ortiz, J. V.; Baboul, A. G.; Stefanov, B. B.; Liu, G.; Liashenko, A.; Piskorz, P.; Komaromi, I.; Gomperts, R.; Martin, R. L.; Fox, D. J.; Keith, T.; Al-Laham, M. A.; Peng, C. Y.; Nanayakkara, A.; Challacombe, M.; Gill, P. M. W.; Johnson, B.; Chen, W.; Wong, M. W.; Andres, J. L.; Gonzalez, C.; Head-Gordon, M.; Replogle, E. S.; Pople, J. A. *Gaussian 98*, revision A. 11.3; Gaussian, Inc.: Pittsburgh, PA, 2002.
(15) (a) Becke, A. D. *J. Chem. Phys*. **1993**, *98*, 5648. (b) Lee, C.; Yang, W.; Parr, R. G. *Phys. Rev. B* **1998**, *37*, 785. (c) Vosko, S. H.; Wilk, L.; Nusair, M. *Can. J. Phys*. **1980**, *58*, 1200.
(16) Hehre, W. J.; Radom, L.; Scheleyer, P. v. R.; Pople, J. A. *Ab Initio Molecular Orbital Theory*; Wiley: New York, 1986; p 76 and references therein.
(17) Hay, P. J.; Wadt, W. R. *J. Chem. Phys*. **1985**, *82*, 299.
(18) McIver, J. W.; Komornicki, A. K. *J. Am. Chem. Soc*. **1972**, *94*, 2625.

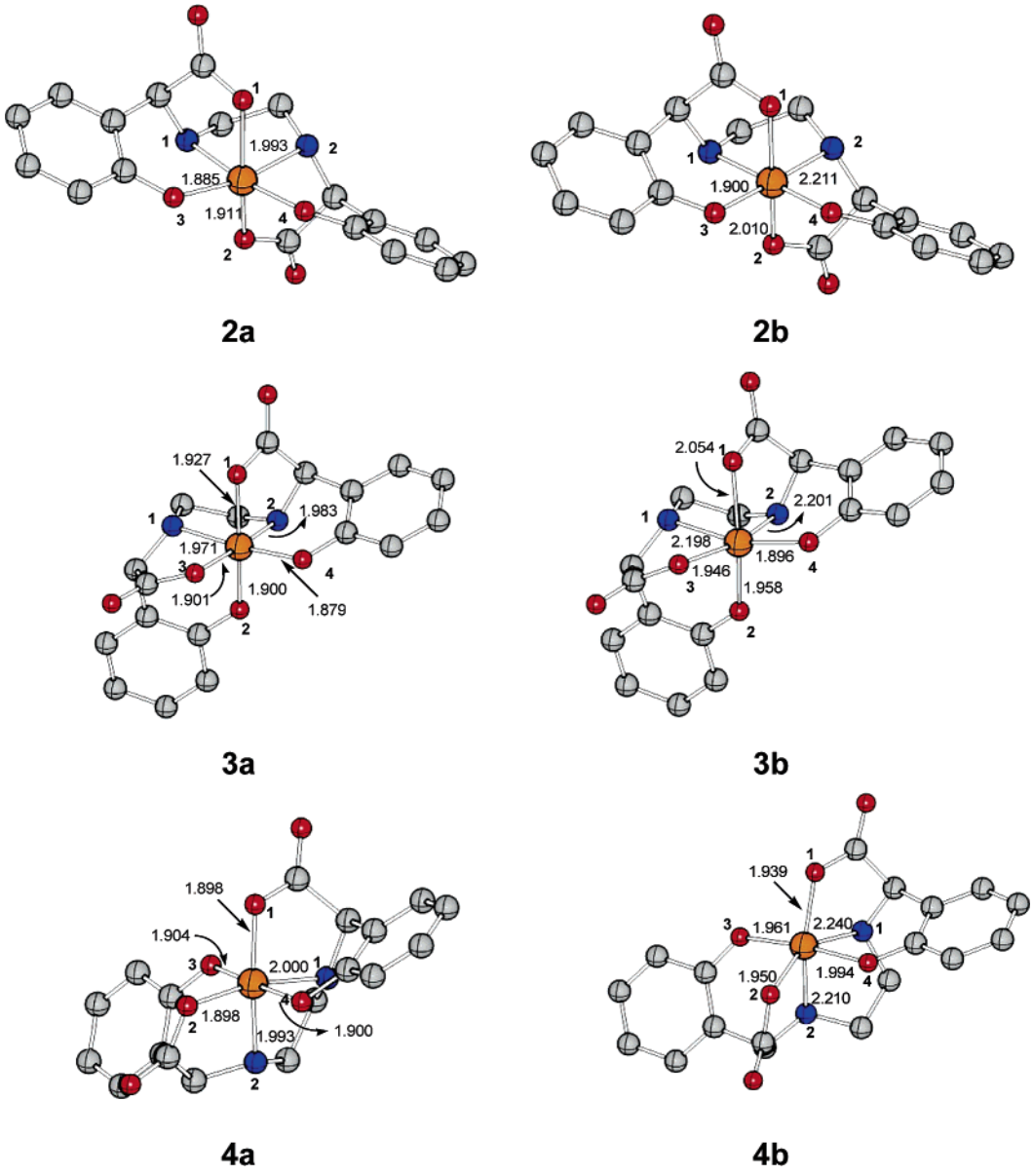

Figure 1. Ball and stick representations of complexes **2a**, **2b**, **3a**, **3b, 4a**, and **4b** (hydrogen atoms were omitted for clarity). All structures correspond to fully optimized B3LYP/6-31G*&LanL2DZ//B3LYP/3-21G*&LanL2DZ geometries. Bond distances are given in Å. Unless otherwise stated, gray, red, blue, and orange colors denote carbon, oxygen, nitrogen, and iron atoms, respectively. **2a** (racemic, $S = {}^1/_2$); **3a** (meso, $S = {}^1/_2$); **2b** (racemic, $S = {}^5/_2$); **3b** (meso, $S = {}^5/_2$); **4a** ([5,5,5] complex, $S = {}^1/_2$); **4b** ([5,5,5] complex, $S = {}^5/_2$).

Table 1. Selected Bond Distances (Å) and Angles (deg) for Complexes **2a**, **2b**, **3a**, **3b**, **4a**, and **4b** for Atoms (for numbers, see Figure 1)

	2a	**2b**	**3a**	**3b**	**4a**	**4b**	racemic[a]	meso[a]
Fe−O1	1.911	2.010	1.927	2.054	1.898	1.939	2.029	2.088
Fe−O2	1.911	2.010	1.900	1.958	1.898	1.950	2.029	2.012
Fe−O3	1.885	1.900	1.901	1.946	1.904	1.961	1.903	1.921
Fe−O4	1.885	1.900	1.879	1.896	1.900	1.994	1.903	1.893
Fe−N1	1.993	2.211	1.971	2.198	2.000	2.240	2.151	2.139
Fe−N2	1.993	2.211	1.983	2.201	1.993	2.210	2.151	2.157
O1−Fe−O2	161.5	152.1	164.2	157.9	101.5	130.1	172.1	172.1
O3−Fe−O4	91.2	111.3	96.6	119.8	87.1	93.8	107.2	112.7
N1−Fe−N2	90.4	81.1	90.7	79.6	81.9	71.1	80.6	79.2
N1−Fe−O4	178.6	164.6	173.6	160.7	81.1	80.1	162.2	168.7
N2−Fe−O3	178.6	164.6	172.8	155.7	85.9	78.5	162.2	154.5

[a] Experimental data for racemic and meso complexes are taken from ref 7.

complex is in full agreement with the values of their stability constants in solution (see above).

The computational data obtained for the [5,5,5] *racemic*-Fe(III)-EDDHA complex in low and high-spin (**4a** and **4b**,

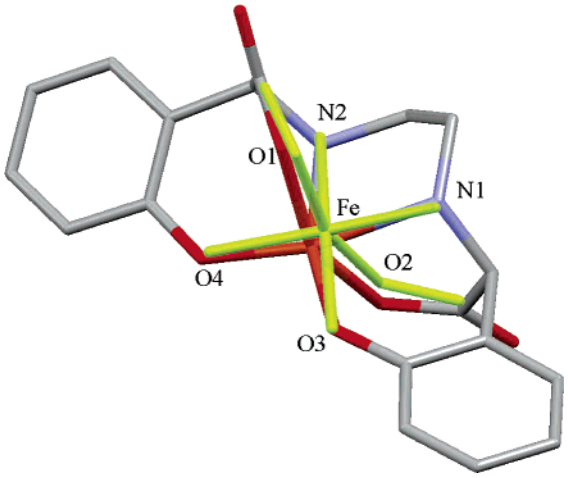

Figure 2. Schematic plot of complexes **2b**, red lines, and **2a**, green lines, showing the shift in $[FeO_4N_2]$ with the change in spin.

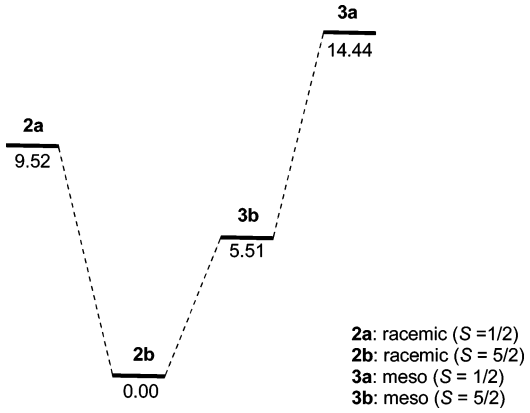

Figure 3. Relative energies (kcal/mol) of complexes **2** and **3**. All values have been computed at the B3LYP/6-31G*&LanL2DZ//B3LYP/3-21G*&LanL2DZ + ΔZPVE level.

respectively) confirm the lower stability of this arrangement and justify why it has not been detected in the crystalline form (Table 1 and Figure 1). The calculated energies of **4a** and **4b** compared to the most-stable high-spin complex **2b** are 30.41 kcal mol^{-1} and 16.67 kcal mol^{-1}, respectively. These values are considerably higher than those of the racemic and meso complexes. Also, in this case, the high-spin complex is considerably more stable than the low-spin one.

The results obtained by DFT calculations about the more-favorable ground spin states were compared with those obtained by solid-state magnetic susceptibility measurements on powdered samples of *meso*- and *racemic*-Na[Fe(III)-EDDHA] complexes. The magnetic moments of both isomers follow the Curie law above 15 K with values around 5.9 β (equivalent to χT values of 4.35 cm^3 K mol^{-1}), typical of an isolated high-spin iron(III) ion (S= 5/2). Below 15 K, there is an abrupt descent in the magnetic moment values, as shown for the racemic complex in Figure 4 (for details of the temperature dependence of χT for the meso isomer see the Supporting Information). This fact can be attributed to an anisotropic distortion of the iron(III) environment, which results in a zero-field splitting of the ground state.[19] Equation 1 for the average magnetic susceptibility takes into account

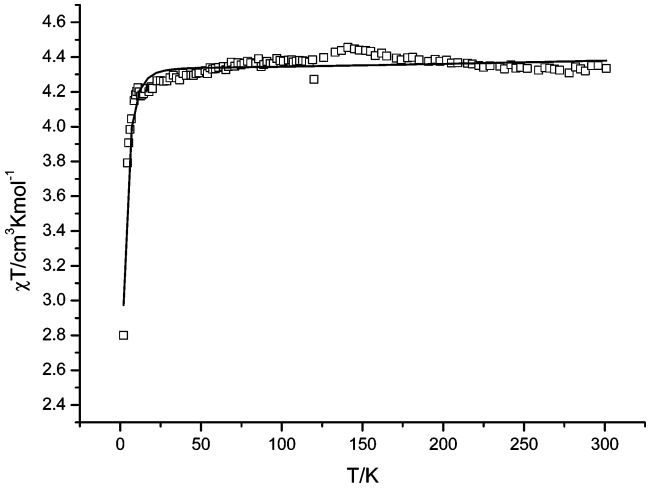

Figure 4. Temperature dependence of χT for the racemic Na[Fe(III)-EDDHA] isomer. The solid line represents the best fit using eq 1 as described in the text.

this single-ion anisotropy, where g_{Fe} is the Landé g factor for the iron ion, k_B is Boltzmann's constant, β is the Bohr magneton, $x = D/k_BT$ with the parameter D measuring the zero-field splitting and $N\alpha$ is the temperature-independent paramagnetism.

$$\langle\chi\rangle = \frac{Ng_{Fe}{}^2\beta^2}{12k_BT}\frac{19 + 16/x + (9 - 11/x)e^{-2x} + (25 - 5/x)e^{-6x}}{1 + e^{-2x} + e^{-6x}} \quad (1)$$

The best fit was obtained when $g_{Fe} = 1.844$, $D = 2.97$ cm^{-1}, and $N\alpha = 2.1 \times 10^{-4}$ cm^3 mol^{-1} for the racemic complex and 1.752, 2.96 cm^{-1}, and 3×10^{-4} cm^3 mol^{-1}, respectively, for the meso isomer. The g_{Fe} values obtained in the fitting are somewhat low, a fact that has been attributed by us to the presence of small quantities of diamagnetic impurities, because the synthetic procedure followed in the preparation of both isomers affords the desired compound accompanied by small quantities of NaCl that cannot be fully removed from the sample. Typical g_{Fe} values are found in the 1.93−2.03 range,[19] suggesting that the diamagnetic impurity corresponds to 10−17% of the racemic sample and 18−25% of the meso sample. These data fit well with the analysis of the purity of *meso*- and *racemic*-Na[Fe(III)-EDDHA] complexes made by the method of Lucena.[20] The obtained fitting values are, nevertheless, typical of slightly distorted octahedral high-spin Fe(III) environments. This observation agrees with the predicted high-spin state for the iron atom obtained for **2** and **3** in the DFT calculations.

The calculated Fe spin densities for the compounds studied are collected in Table 2. The correlation diagram of the SOMOs of the most-stable high-spin (S = 5/2) Fe(III) complex **2b** as well as the plot of the corresponding orbitals are shown in Figure 5. According to the diagram, the electron

(19) (a) Khan, O. *Molecular Magnetism*; VCH: New York, 1993; pp 23−26. (b) Carlin, R. L. *Magnetochemistry*; Springer-Verlag: Berlin, 1986; p 55.

(20) (a) Lucena, J. J.; Barak, P.; Hernández-Apaolaza, L. *J. Chromatogr., A* **1996**, 727, 349. (b) Hernández-Apaolaza, L.; Barak, P.; Lucena, J. J. *J. Chromatogr., A* **1997**, *789*, 453.

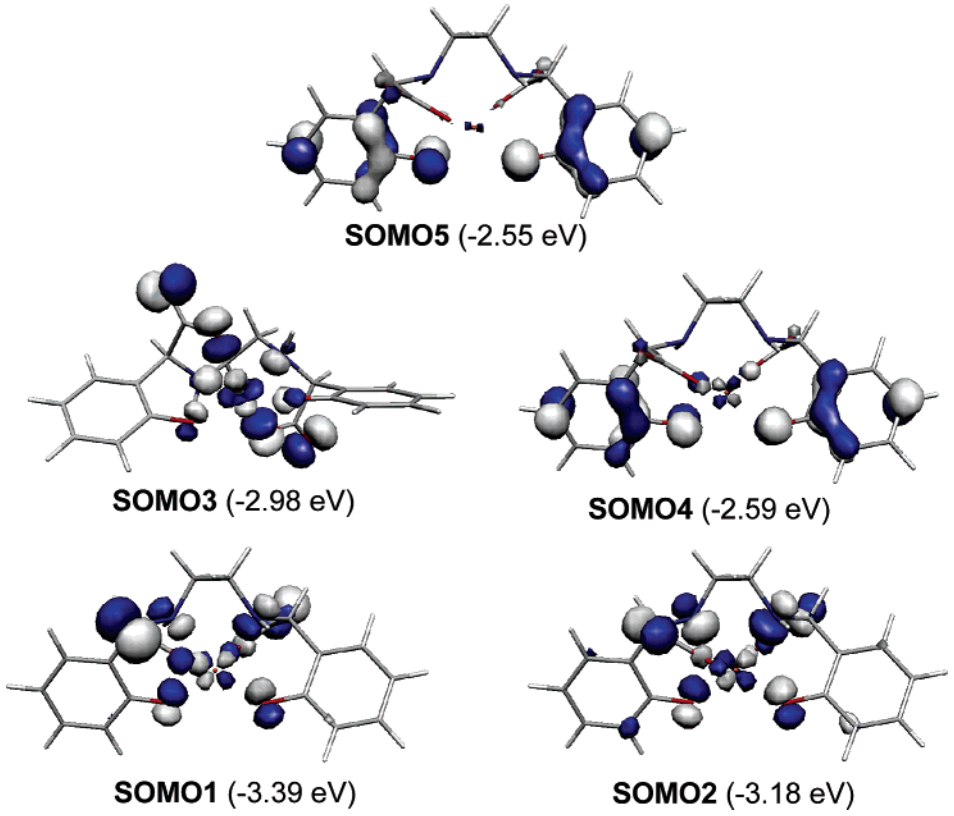

Figure 5. Energy values (eV) of the d orbitals and SOMOs of complex **2b**. All values have been computed at the B3LYP/6-31G*&LanL2DZ//B3LYP/3-21G*&LanL2DZ + ΔZPVE level.

Table 2. Spin Densities (B3LYP/6-31G*&LanL2dz//B3LYP/3-21G*&LanL2dz) of the Fe atom in Racemic and meso *O,O*-EDDHA Fe(III) Complexes **2** and **3**

complex	Fe spin density
2a ($S = {}^1/_2$)	0.937
2b ($S = {}^5/_2$)	4.015
3a ($S = {}^1/_2$)	0.948
3b ($S = {}^5/_2$)	4.016

configuration of **2b** is $(d_{xz})^1\ (d_{yz})^1\ (d_{x^2})^1\ (d_{xy})^1\ (d_{x^2-y^2})^1$, which fits with the distorted octahedral geometry of the complex.[21] However, the spin density calculated on the iron atom (Table 2) corresponds to only four electrons. This fact could be explained by considering the SOMOs also displayed in Figure 5. The plot indicates that the four lower-energy orbitals show a noticeable participation of the iron d orbitals, whereas the highest energy SOMO is better described as a ligand-based orbital.

We have already mentioned that high-spin Fe(III) porphyrins are reluctant to take part in photochemically induced ET reactions.[12] As stated above, Fe(III)-EDDHA complexes are unreactive in ET processes, promoted by either light (photodegradation) or chemical ET reagents.[11] It is believed that the photodegradation of Fe(III) polycarboxylate complexes (i.e., oxalates and citrates) requires the initial reduction of the Fe(III) in a ligand-to-metal photoinduced single-electron-transfer process (SET).[22] Considering the above precedents, the presence of a high-spin ($S = 5/2$) iron in Fe(III)-EDDHA complexes could hamper the ET process, enhancing other deactivation pathways for the excited molecule. The reluctance of these complexes toward reduction is also evident when the electron transfer to the Fe(III) is promoted by chemical reagents or under electrochemical conditions.

Conclusions

Computational studies have shown that the *racemic*-Fe(III) EDDHA complex is more stable than the meso isomer, regardless of the spin state of the central iron atom. A comparison of the energy values obtained for the complexes under study has also shown that high-spin ($S = 5/2$) complexes are more stable than low-spin ($S = 1/2$) ones. This fact has been confirmed experimentally by the magnetic susceptibility values of both isomers. In both cases, their behavior has been fitted as being due to isolated high-spin Fe(III) in a distorted octahedral environment. The study of the correlation diagram also confirms the high-spin iron in complex **2b**. The mean angles and bond distances obtained through DFT calculations for compounds **2b** and **3b** are fully in agreement with those reported for the X-ray data of the reported crystal structures. Considering the previous studies in porphyrins, the presence of a high-spin iron in Fe(III)-EDDHA complexes could be the key to understanding their lack of reactivity in electron-transfer processes, either

(21) It is known that the occupation of the antibonding (e_g) set in high-spin Fe complexes causes the elongation of the axial iron ligand bonds, and in other cases, the extrusion of the Fe out of the equatorial plane of the complex has also been reported (see ref 2a).

(22) Faust, B. C.; Zepp, R. G. *Environ. Sci. Technol*. **1993**, *27*, 2517.

chemically or electrochemically induced, and their resistance to photodegradation. As expected, the computational data obtained for the [5,5,5] *racemic*-Fe(III)-EDDHA complex confirm the low stability of this arrangement and justify why it has not been detected in the crystalline form. Also in this case, the high-spin complex is considerably more stable than the low-spin one. On the basis of these results, we can affirm that the geometry optimization of these complexes performed with the standard 3-21G* basis set for hydrogen, carbon, oxygen, and nitrogen and the Hay-Wadt small-core effective core potential (ECP) including a double-ξ valence basis set for iron, followed by single-point energy refinement with the 6-31G* basis set, is suitable for predicting both the geometries and the spin-states of EDDHA-Fe(III) complexes.[23] Therefore, these computational tools are, in principle, appropriate for further investigations in understanding the mechanism of iron uptake by plants. Efforts toward these goals are now in progress in our laboratories.

Acknowledgment. Financial support by the Spanish Ministerio de Ciencia y Tecnología (CTQ2004-06250) is gratefully acknowledged. I.F. thanks the Ministerio de Educación y Ciencia for a predoctoral fellowship.

Supporting Information Available: Plot of the temperature-dependence of χT for the *meso*-Na[Fe(III)-EDDHA] isomer and Cartesian coordinates and total energies for all stationary points discuess in text. This material is available free of charge via the Internet at http://pubs.acs.org.

IC0520723

(23) Although the standard triple-ξ plus polarization set is commonly used in DFT studies of transition-metal complexes, there are several examples of the use of a double-ξ polarization set in these cases. Recent examples on the use of the triple-ξ plus polarization set: (a) Han, W.-G.; Liu, T.; Lovell, T.; Noodleman, L. *J. Am. Chem. Soc.* **2005**, *127*, 15778. (b) Dey, A.; Chow, M.; Taniguchi, K.; Lugo-Mas, P.; Davin, S.; Maeda, M.; Kovacs, J. A.; Odaka, M.; Hodgson; K. O.; Hedman, B.; Solomon, E. I. *J. Am. Chem. Soc*. **2006**, *128*, 533. (c) Dey, A.; Roche, C. L.; Walters, M. A.; Hodgson, K. O.; Hedman, B.; Solomon, E. I. *Inorg. Chem.* **2005**, *44*, 8349. Recent examples on the use of double-ξ: (d) Bhattacharya, D.; Dey, S.; Maji, S.; Pal, K.; Sarkar, S. *Inorg. Chem.* **2005**, *44*, 7699. (e) Iwakura, I.; Ikeno, T.; Yamada, T. *Angew. Chem., Int. Ed.* **2005**, *44*, 2524. (f) de Visser, Sam P. *Angew. Chem., Int. Ed.* **2006**, *45*, 1790. (g) Nakashima, H.; Hasegawa, J.-Y.; Nakatsuji, H. *J. Comput. Chem.* **2006**, *27*, 426. (h) Jelovica, I.; Moroni, L.; Gellini, C.; Salvi, P. R. *J. Phys. Chem. A* **2005**, *109*, 9935.